JOURNAL OF GEOPHYSICAL RESEARCH, VOL. 112, G04S08, doi:10.1029/2006JG000321, 2007

Life in the Atacama: A scoring system for habitability and the robotic exploration for life

Andrew N. Hock,[1] Nathalie A. Cabrol,[2,3] James M. Dohm,[4] Jennifer Piatek,[5] Kim Warren-Rhodes,[2,3] Shmuel Weinstein,[6] David S. Wettergreen,[7] Edmond A. Grin,[2,3] Jeffrey Moersch,[5] Charles S. Cockell,[8] Peter Coppin,[9] Lauren Ernst,[6] Gregory Fisher,[6] Craig Hardgrove,[5] Lucia Marinangeli,[10] Edwin Minkley,[6] Gian Gabriele Ori,[10] Alan Waggoner,[6] Mike Wyatt,[5] Trey Smith,[7] David Thompson,[7] Michael Wagner,[7] Dominic Jonak,[7] Kristen Stubbs,[7] Geb Thomas,[11] Erin Pudenz,[11] and Justin Glasgow[11]

Received 20 September 2006; revised 6 July 2007; accepted 21 November 2007; published 29 December 2007.

[1] The science goals of the Life in the Atacama (LITA) robotic field experiment are to understand habitat and seek out life in the Atacama Desert, Chile, as an analog to future missions to Mars. To those ends, we present a new data analysis tool, the LITA Data Scoring System (DSS), which (1) integrates rover and orbital data relevant to environmental habitability and life detection, and (2) provides a standard metric, or ''score'' to evaluate (a) the potential habitability, and (b) the strength of evidence for life at all locales along the rover's traverse. Designed and tested during the 2005 field campaign, first results from the DSS indicate that the three selected sites in the Atacama Desert are generally inhospitable. The strength of evidence for life is positively correlated with potential habitability at two of the three sites. Using factor analysis, we find three factors explain 79.9% of the variance in biological observations and five factors explain 96.2% of the variance in potential habitability across all sites. These factors are used to focus a discussion of scoring variable definitions for future robotic missions in the Atacama and of instrument selection and strategy development for future robotic missions on Earth and Mars.

Citation: Hock, A. N., et al. (2007), Life in the Atacama: A scoring system for habitability and the robotic exploration for life, *J. Geophys. Res.*, *112*, G04S08, doi:10.1029/2006JG000321.

1. Introduction

[2] The Life in the Atacama (LITA) experiment employs a highly mobile rover to characterize the distribution of habitats and life in the Atacama Desert, one of the world's driest and most inhospitable environments. The rover, Zoë, is remotely operated by a science team under conditions simulated by a robotic mission to Mars. Building upon the technology employed by previous terrestrial rovers such as Rocky 7 [*Arvidson et al.*, 1998], Nomad [*Wettergreen et al.*, 1999; *Cabrol et al.*, 2001a, 2001b], FIDO [*Arvidson et al.*, 2002], and Marsokhod [*Stoker et al.*, 2001], Zoë has the capability to observe not only aspects of geology and climate [*Wettergreen et al.*, 2005a, 2005b], but also to make direct observations of life [e.g., *Weinstein et al.*, 2006]. The project's first two field seasons, 2003 and 2004, focused on technology demonstration, testing the robotics and integrating instrumentation and controls. Following these and anticipating the science requirements of future missions to Mars, a central goal of the 2005 campaign was to identify and characterize locales of elevated potential habitability within and across the landing ellipses defined for three tests sites of varying environmental conditions (sites D, E, and F; see *Warren-Rhodes et al.* [2007a, 2007b] for further discussion). A locale is defined in this study as any location subject to targeted investigation by the rover. Since orbital and field data sets employed in the pursuit of this goal are valid on different spatial scales, a tier-scalable approach was taken: orbital data was used to constrain hypotheses regarding the potential habitability of regions within each site's

[1]Department of Earth and Space Sciences, University of California, Los Angeles, Los Angeles, California, USA.
[2]Space Science Division, NASA Ames Research Center, Moffett Field, California, USA.
[3]SETI Institute, Mountain View, California, USA.
[4]Hydrology and Water Resources Department, University of Arizona, Tucson, Arizona, USA.
[5]Department of Earth and Planetary Sciences, University of Tennessee, Knoxville, Tennessee, USA.
[6]Molecular Biosensor and Imaging Center, Mellon Institute, Carnegie Mellon University, Pittsburgh, Pennsylvania, USA.
[7]Robotics Institute, Carnegie Mellon University, Pittsburgh, Pennsylvania, USA.
[8]Planetary and Space Sciences Research Institute, Open University, Milton Keynes, UK.
[9]Eventscope, Remote Experience and Learning Laboratory, Studio for Creative Inquiry, Carnegie Mellon University, Pittsburgh, Pennsylvania, USA.
[10]International Research School of Planetary Sciences, Pescara, Italy.
[11]GROK Laboratory, University of Iowa, Iowa City, Iowa, USA.

0148-0227/07/2006JG000321$09.00

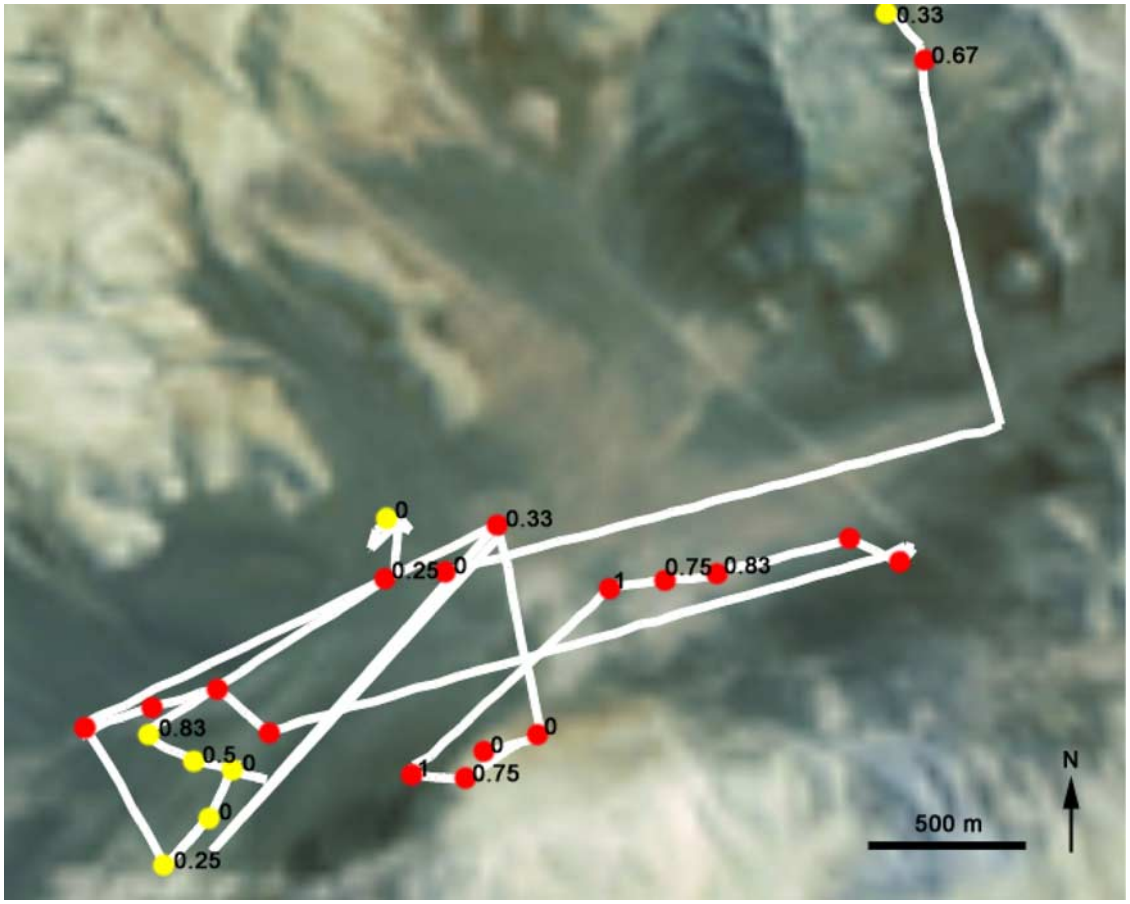

Figure 1. The site D rover traverse, illustrating a representative map product of the DSS. Investigated locales are indicated by push-pin icons. Each pin is color-coded to indicate its environmental score (or potential habitability, see section 3 of the text for details): yellow indicates an intermediate habitability rating, red indicates low habitability, and highly habitable locales, which would be green, are not found. Each pin is also enumerated: (1) in white with the biology score ratio that indicates the strength of evidence for life ranging between 0–1; (2) in the color of the respective pin with the locale's identifying information. This map was generated during mission operations for on the fly data visualization and planning. All image data are produced using Eventscope software (details given by P. Coppin et al. (unpublished manuscript, 2007)). An ASTER false color visible-band image and digital elevation model provide the background color and texture (NASA/JPL).

landing ellipse on the kilometer scale and thus target the rover's midterm to long-term exploration strategy on day to multiday timescales. Field data acquired by the rover was used to evaluate those hypotheses, make daily plans and alter longer-term exploration strategy where needed.

[3] This novel goal of robotic exploration requires a better understanding of how environmental factors influence habitability in a desert ecosystem such as the Atacama and, importantly, how they relate to the presence or remote detection of life. With this in mind, we set out to create a data analysis tool, named the Data Scoring System (DSS), for the LITA experiment with the following goals: (1) Integrate data collection relevant to habitable environments and distribution of life in the Atacama Desert. (2) Provide a standard metric to evaluate and map (a) the potential habitability, and (b) the evidence for life at all locales using available data. Figure 1 shows a representative

[4] Table 1 depicts the relevance of the scoring system within the larger framework of the project's scientific objectives, while Figure 1 provides a representative example of a DSS mapping product. Here, we present the design and first implementation of the DSS during the 2005 LITA campaign. The LITA DSS is defined by two sets of variables, environmental and biological, chosen based upon the rover's instrument suite and the capabilities of available orbital data. Environmental variables address potential habitability, while biological variables address the strength of evidence for life each targeted locale. There, the rover science team analyzes all relevant, available data and assigns each variable a numeric rating, or score, which ranges from 0–2 (see section 3, below, for detailed methods and definitions).

[5] It is important to note here that the design and implementation of this scoring system are experimental in nature. Though some scores are traceable to quantitative variation, they are largely qualitative with the intention of illustrating how environmental data may be used to constrain zones of potential habitability and give context to high priority biological investigations. Furthermore, the variables that form the basis of the environmental and

Table 1. Relevance of the LITA DSS to Project Science Objectives[a]

Objectives[a]	Description[a]	DSS Relevance
Seek Life	Establish if the hyperarid region of the Atacama represents an absolute limit to life and understand the gradient of biodiversity and environments	(a) Integrates results from biological analyses (b) Biology score provides a standard metric to compare, map results between sites and amongst locales
Understand Habitat	Understand the strategies used by life to survive in arid environment following climate changes	(a) Integrates results from environmental analyses (b) Paired with biology score, enables evaluation of hypotheses regarding habitability between sites and amongst locales
Apply Relevant Science	Design a payload capable of identifying environments for life and test science exploration strategies enabling the positive identification of life	(a) Production of a standard data product to study the relationship between habitability and life detection (b) Enables subsequent results-driven payload development for terrestrial desert rovers and rovers for planetary (Mars) exploration

[a]Objectives and description from *Wettergreen et al.* [2005b]; additional engineering objectives of the project are discussed therein.

biological elements of the scoring system should not be considered an exhaustive list, as the DSS will be updated depending on the science objectives, environmental conditions of the planetary body to be explored, and the payload-defined data availability [e.g., *Fink et al.*, 2005; *Schulze-Makuch et al.*, 2005]. Additionally, they are tailored to Zoë's study of near-surface, terrestrial life and its habitability in the Atacama Desert. This search targets organisms present in the upper centimeters of soil by the presence of terrestrial biomarkers such as proteins, carbohydrates, lipids, DNA and chlorophyll, or by the morphology of known terrestrial organisms such as lichens and small plants. The metrics of habitability also contain terrestrial biases, including but not limited to constraint by surface water flow or those indicated by the presence of chlorophyll. Therefore, application of the DSS to Mars exploration is not direct, but rather this work represents a critical first step in understanding the processes governing habitability and robotic life detection under more controlled conditions. For example, putative candidate sites of extinct or possibly extant hydrothermal activity on Mars, as targets of elevated biological potential, would require modified definitions of habitability, life and appropriately modified variable definitions [e.g., *Dohm et al.*, 2004; *Furfaro et al.*, 2006; *Schulze-Makuch et al.*, 2007].

[6] In the following sections, we provide a detailed account of the design and implementation of the DSS, presenting numerical results from and statistical analysis of its application across sites D, E, and F of the 2005 LITA field campaign. We first illustrate the resultant relationship between habitability, as modeled by the scoring system, and bioloical findings from the rover's fluorescence imager (see *Weinstein et al.* [2007] for details). Second, we investigate the correlation between individual environmental variables and biological results. Last, we perform factor analysis to identify the factors underlying variation in habitability and biology in the Atacama and screen the variables employed in this first use of the scoring system for future rover missions on Earth and beyond to Mars.

2. General Methods

2.1. Field Sites

[7] The 2005 campaign of the LITA experiment investigated life and its habitats at three sites in the Atacama (sites D, E, and F as illustrated in Figure 2). The Atacama Desert was selected for this rover field experiment because it bears several environmental and geological analogies to Mars: (1) arid, low temperature desert conditions, (2) magma-water interactions and other hydrothermal activity, (3) evidence of tectonic processes, including fracturing, faulting, and basin formation, (4) presence of analogous materials, including igneous mineralogy and thick evaporite sequences, (5) structurally controlled basins and collapse-related depressions, (6) landscape features related to aqueous processes such as sapping channels and alluvial fans, (7) landscape features related to climate-driven aqueous processes such as flood-carved terrain and dry lakebeds [e.g., *Mouginis-Mark*, 1985, 1990; *Baker et al.*, 1991; *Scott et al.*, 1993, 1995; *Tanaka et al.*, 1998, 2005; *Chong Diaz et al.*, 1999; *Dohm et al.*, 2001a, 2001b, 2001c, 2004; *Cabrol et al.*, 2001b, 2007; *Baker*, 2001; *Christensen et al.*, 2001; *Fairén et al.*, 2003; *Neukum et al.*, 2004; *Márquez et al.*, 2004; *Squyres et al.*, 2004; *Gendrin et al.*, 2005; *McSween et al.*, 2006; *Warren-Rhodes et al.*, 2007a, 2007b; *Schultze-Makuch et al.*, 2007]. The specific study sites within the Atacama were chosen to represent a spectrum of habitability, generally constrained by relative abundance of liquid water delivered to putative near-surface habitats by fog, clouds, and potentially rain/snowfall. Site D, due to its coastal proximity and climate, had the highest potential for delivery of water by these means. Moving inland, site E was located within the Atacama's hyperarid core and was chosen to represent a significantly drier climate. Still further inland, site F, near the Andean Pre-Cordillera, was selected to represent the most arid and thus perhaps the most inhospitable environment of the three sites.

2.2. Operations

[8] The general schedule of operations began with prelanding analysis of orbital data. The science team was given orbital data relevant to a ~20 km x 10 km "landing ellipse" chosen to roughly approximate the landing error of future landed Mars missions and constrain prelanding analysis. Within this ellipse, the team worked to identify regions of interest based upon (a) past or present aqueous activity as evidenced by geomorphology, (b) the presence of habitats or relict water-bearing environments as evidenced by surface mineralogy, (c) atmospheric water vapor transport and

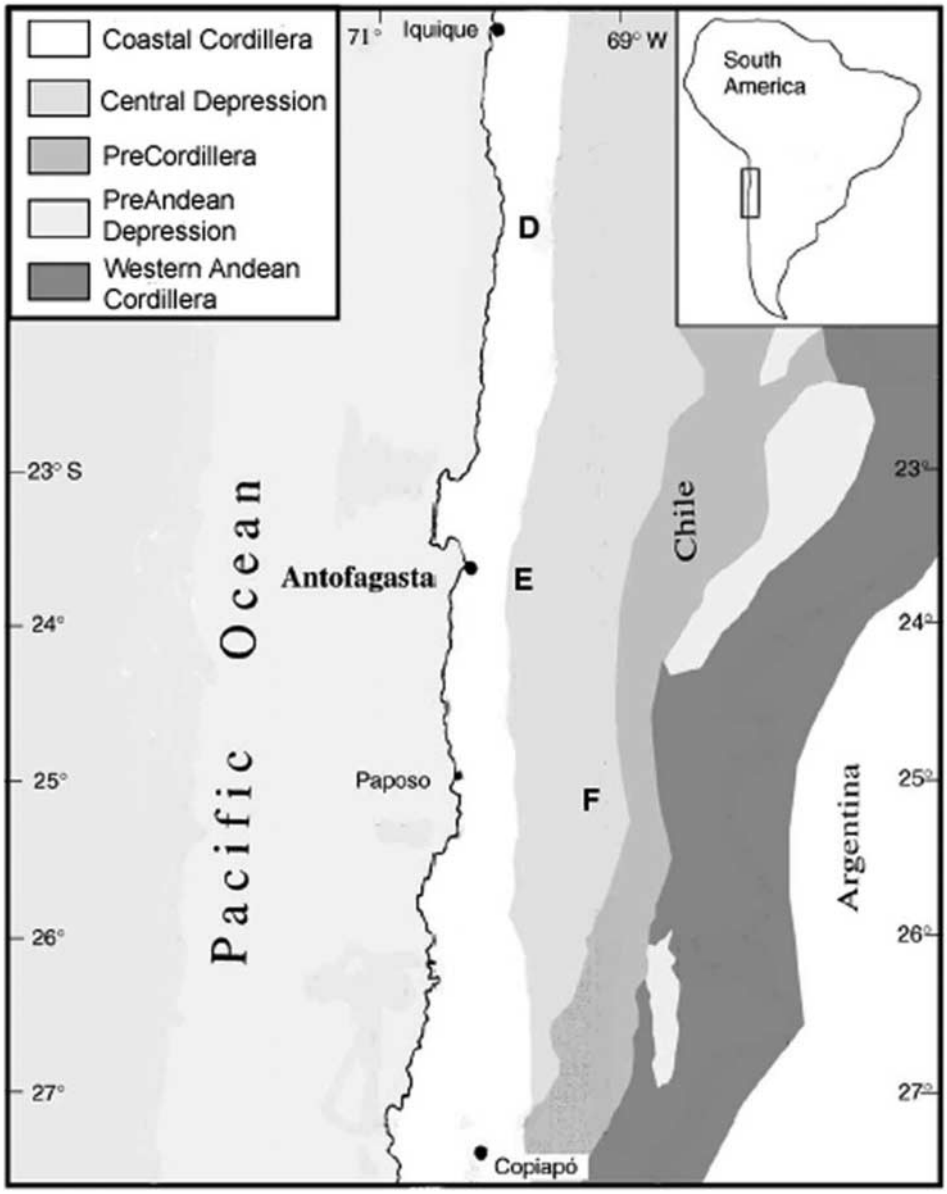

Figure 2. Location map of LITA sites D, E, and F within the general physiography of the Chilean Atacama Desert [following *Riquelme et al.*, 2003; *Warren-Rhodes et al.*, 2007a, 2007b].

potential deposition as evidenced by visible-band imagery and corroborating topography, (d) the direct observation of biosignatures, such as chlorophyll [e.g., *Piatek et al.*, 2007; *Warren-Rhodes et al.*, 2007a]. Following Zoë's safe deployment, or ''landing,'' the team continued to employ orbital data as well as initial panoramas from the rover to locate the rover's position by triangulation. See P. Coppin et al. (unpublished manuscript, 2007), for more information regarding the software tools employed by the Remote Science Operations Team. Daily operations began immediately: commands were sent to the rover, Zoë, on a once-daily basis to mimic the communication constraints of a robotic mission to Mars. Likewise, data downlink from the field occurred once per day and was bandwidth-constrained. Long-term exploration strategy largely followed hypotheses regarding the habitability of environments devised during prelanding analysis, but was updated and reshaped on a daily basis following analysis of rover field data. Conceived during prelanding operations at site D, the first goals of the Data Scoring System were to integrate data from orbital and in situ sources regarding habitability and life to streamline short-term strategy development.

3. Data Scoring System

3.1. Design

[9] The LITA DSS consists of two central elements: environment and biology. In turn, each element is composed of a set of variables that are indicative of the potential habitability and presence of life, respectively, at a given locale. Definition of variables was chosen to maximize utility of the rover's scientific payload, and in turn, maxi-

Table 2. Environmental Variables[a]

Variable	Description/Rationale	Data Source
	Orbital	
1. Atmospheric Water[b]	Presence of fog and/or clouds	Available orbital data (e.g., ASTER, IKONOS)
2. Chlorophyll	Chlorophyll spectral signature	ASTER VNIR spectrometer
3. Evaporite Mineralogy	Sulfate and/or carbonate spectral signature	ASTER TIR surface emissivity
4. Fog Deposition[b]	Presence of potential embankment for atmospheric water (e.g., fog, clouds)	Available orbital data (e.g., ASTER, IKONOS) and derived DEMs
5. Hydrologic Geomorphology[b]	Evidence for paleohydrologic and/or paleohydrogeologic activity (e.g., drainages, basins, polygons, sapping channels, mud cracs, structurally controlled releases of water)	Available orbital data (e.g., ASTER, IKONOS)
6. Quartz	Quartz spectral signature	ASTER TIR surface emissivity
	Field	
7. Bound/Interlayer Water	Bound/interlayer water and/or hydrated mineral spectral signature	VNIR spectrometer, linear deconvolution
8. Chlorophyll	Chlorophyll spectral signature	VNIR spectrometer
9. Evaporite Mineralogy	Sulfate and/or carbonate spectral signature	VNIR, TIR Spectrometer
10. Fog Deposition (regional)[b]	Potential for atmospheric water deposition indicated by topography	SPI, orbital digital elevation map (DEM)
11. Hydrologic Geomorphology[b]	Evidence for paleohydrologic and/or paleohydrogeologic activity (e.g., drainages, basins, polygons, mud cracks)	SPI, navcam
12. Insolation[b]	Shelter/shade from intense solar radiation	SPI, navcam, EnviS (solar pyranometer)
13. Moisture (locale)[b]	Visible evidence for moisture (e.g., condensed or ponded water)	All visible-band cameras
14. Moisture (regional)[b]	Visible identification of regional-scale moisture (e.g., distant hills with fog, snow-capped mountains)	SPI
15. Promising Habitat[b]	Visible identification of "promising" habitat, as defined by user experience	All visible-band cameras
16. Quartz	Quartz spectral signature	TIR
17. Relative Humidity	Elevated overnight relative humidity	EnviS (RH sensor)
18. Water Vapor Condensation	Atmospheric water condensation on surface	EnviS (leaf wetness, air temperature sensor)

[a]Implementation and scoring procedure is described in section 3.2 of the text. Data sources are described in further detail by *Piatek et al.* [2007]: ASTER, IKONOS, derived digital elevation models and *Cabrol et al.* [2007]: rover TIR and VNIR spectrometer, SPI and navigational cameras (navcam), and environmental sensors (EnviS).

[b]This variable is not quantified in this study.

mize the opportunity for correlation among variables that bear on environmental habitability and those that indicate the actual presence of life. The habitability of a given environment is a function of many factors, most notably those related to local energy and nutrient flux, physical and chemical properties of the substrate, and the availability of liquid water. Following the LITA project science goals, Zoë's payload [*Cabrol et al.*, 2007] includes several instruments capable of characterizing these: (1) a visible, near infrared (VNIR) spectrometer, (2) a thermal infrared (TIR) spectrometer, (3) environmental sensors (EnviS) for air temperature and relative humidity, and leaf wetness, (4) a suite of visible-band cameras, including stereo panoramic imagers (SPI), workspace and navigational cameras (navcams). To the same ends, the remote science team was given access to orbital data including visible, near infrared and thermal infrared imagery from the Advanced Spaceborne Thermal Emission and Reflectivity Radiometer (ASTER – NASA/JPL) and high resolution panchromatic (visible-band) imagery from IKONOS (orbital data described in more detail by *Piatek et al.* [2007]). The eighteen variables of the DSS that follow from this, divided by their means of acquisition, are shown in Table 2. Collectively, they contain information about (1) the presence, transport, and bioavailability of atmospheric water vapor, (2) the presence and distribution of mineralogy associated with known desert habitats (e.g., evaporites, quartz), (3) the presence and distribution of chlorophyll, (4) geological evidence for past or present aqueous activity, (5) the availability and intensity of solar radiation, and (6) atmospheric water condensation (i.e., the presence of dew).

[10] Life detection using Zoë is made possible using the onboard fluorescence imager (FI) [*Wettergreen et al.*, 2005a, 2005b; *Weinstein et al.*, 2006, 2007]. The six biology variables shown in Table 3 are used to score the strength of evidence for life at each locale. Five of the six biology variables are objectively determined, following directly from representative images of biomolecule fluorescence (i.e., carbohydrate, chlorophyll, DNA, lipid and protein). Morphology, on the other hand, is the subjective identification of a life form only by its shape: this variable follows qualitatively from color images of the FI or other visible band cameras.

3.2. Implementation

[11] Upon the receipt of new observational data from the rover, attention in the Remote Science Operations facility turned to scoring. Daily downloaded data was reviewed locale by locale (for each rover stop and investigation). Team members with relevant experience were chosen to spearhead data analysis for a given set of variables and propose scores for each at each locale. Proposed scores were

Table 3. Biology Variables[a]

Variable	Description/Rationale	Data Source
1. Morphology[b]	Direct observation of morphology indicative of extant life	SPI, Navcams, Workspace Cams, FI
2. Carbohydrate	Biology indicated by carbohydrate fluorescence	FI
3. Chlorophyll	Biology indicated by chlorophyll fluorescence	FI
4. DNA	Biology indicated by DNA fluorescence	FI
5. Lipid	Biology indicated by lipid fluorescence	FI
6. Protein	Biology indicated by protein fluorescence	FI

[a]Implementation and scoring procedure is described in section 3.2 of the text. Data sources are described in further detail by *Weinstein et al.* [2007]: fluorescence imager (FI) and *Cabrol et al.* [2007]: SPI, workspace and navigational cameras (navcams).
[b]This variable is not quantified in this study.

then reviewed by the entire team and entered to a database. The possible score for any one variable at a given locale has an integer range from 0 to 2: in general, 0 indicates support of the null hypothesis (no evidence for habitability, no evidence for life), while a score of 2 refutes the null hypothesis, or lends credence to the hypothesis that a given environment is habitable or shows strong evidence for life. In a preliminary version of the DSS, a binary scoring system was proposed (there, a score of 0 indicated uninhabitable, no life and a score of 1 indicated habitable, life present), but ambiguous data or weak signals in some cases demanded the inclusion of an intermediate value. In cases of missing or faulty data, or where no observation was recorded or applicable, no score was assigned and that variable was not accounted for in the total score for the respective locale. The specific observations employed in the scoring of each variable listed in Tables 2 and 3 are detailed in sections 3.2.1 and 3.2.2 below. Additional methods pertaining to specific data may be found as follows: orbital and spectral analysis [*Piatek et al.*, 2007], geological and geomorphologic analysis, and biological analysis [*Warren-Rhodes et al.*, 2007a, 2007b; *Weinstein et al.*, 2007].

3.2.1. Scoring Environmental Variables

[12] As in Table 2, the eighteen environmental variables discussed here are divided by their means of acquisition: (a) orbital, and (b) field, or rover-acquired data. An asterisk following the variable name indicates that its evaluation for the purposes of this study were not quantitative. For each entry, the required data set(s) is listed, and followed by a definition of score values ranging from 0 to 2 with notes, where applicable.

3.2.1.1. Orbitally Derived Environmental Variables

[13] 1. Atmospheric Water* – Data set required: orbital visible-band imagery. 0 = No water (e.g., clouds, fog) is visible in orbital imagery. 1 = Some evidence of clouds or fog in the region/orbital scene, but not directly visible over the locale. 2 = Direct observation of clouds or fog over the locale of interest. Notes: This factor may be biased due to cloud free image selection and the narrow temporal window of observations: only one or two observations were made available at each per site.

[14] 2. Chlorophyll – Data set required: ASTER visible/near infrared (VNIR) orbital imagery. 0 = no signature indicating chlorophyll concentrations. 1 = faint signature of chlorophyll. 2 = intense signature. Notes: ASTER false color image displays ASTER Band 3 (807 nm, NIR) in the red channel, Band 2 (661 nm, red) in the green channel, and Band 1 (556 nm, green) in the blue channel: the resulting image may indicate the presence of chlorophyll. Level1B or Level2 data set required for georeferencing and atmospheric correction.

[15] 3. Evaporite Mineralogy – Data set(s) required: ASTER thermal infrared (TIR) surface emissivity. 0 = Not identified in area. 1 = Sulfates and/or carbonates indicated in low concentrations (<35%) in general area of locale; may also apply where one or two anomalously high concentration pixels are present in an area dominated by other compositions, if RMS error in linear deconvolution results is high, or when blackbody results from deconvolution indicate the presence of minerals with no significant absorption features, such as halite. 2 = High concentrations of sulfates and/or carbonates (>35%). Notes: Emissivity requires Level 2 ASTER processing; the ''mineral mapping'' strategy will not work with L1B data. As with field spectra, certain evaporite minerals, such as halite, have no diagnostic absorption features in the TIR.

[16] 4. Fog Deposition* – Data set(s) required: available orbital imagery and derived topography. 0 = Locales that have little to no potential for moisture embankment such as broad plains with few to no breaks in slope. 1 = Areas, locales, features that may lead to moisture embankment/catchment. 2 = Similar to 1, but potential for deposition in the presence of atmospheric water is increasingly likely.

[17] 5. Hydrologic Geomorphology* – Data set(s) required: Visible-band orbital imagery. 0 = no geomorphic evidence of hydrologic and/or hydrogeologic activity. 1 = some indicators of hydrologic and hydrogeologic activity such as visible paleodrainages in the region. 2 = increased frequency and diversity of hydrologic/hydrogeologic indicators in the region (e.g., drainages, drainage networks, drainages that debouch into topographic lows such as basins, or those resulting from collapse).

[18] 6. Quartz – Data set(s) required: ASTER TIR surface emissivity. 0 = Not identified in area. 1 = Quartz indicated in low concentrations (<35%) in general area of locale. May also apply if other silica minerals (i.e., obsidian) are concentrated in the area, if RMS error in deconvolution is high, or when one or two anomalously high quartz pixels appear in an area that otherwise contains very little or no quartz. 2 = Significant concentrations of quartz (>35%). Notes: as above, emissivity requires Level2 ASTER processing.

3.2.1.2. Field-Derived Environmental Variables

[19] 7. Bound/Interlayer Water – Data set(s) required: VNIR and/or TIR field spectra. 0 = No identifiable water or hydrated mineral absorption features, no hydrated minerals suggested by linear deconvolution. 1 = Shallow absorption features and/or linear deconvolution results indicating concentrations <35%. May be applied when data is very noisy and difficult to analyze, but results suggest a hydrated composition. 2 = Distinct diagnostic absorption features and/or linear deconvolution results indicating concentrations >35%. Notes: 35% delineation arbitrary but greater than 10% where linear deconvolution becomes unreliable.

[20] 8. Chlorophyll – Data set(s) required: VNIR field spectra. 0 = ~500 nm jump in reflectance from visible to NIR not present. 1 = possible increase in NIR reflectivity due to chlorophyll. 2 = definitive identification of chlorophyll via the chlorophyll jump. Notes: The ''jump'' is hard to describe, but it should be a steep and significant increase in reflectivity between the visible and near infrared wavelengths (~500–800 nm): many minerals also exhibit an increase in nearby wavelengths, but it over the same range and does not have the same magnitude. A score of one in this work is unlikely due to inherent binary nature of this factor, although it could apply for noisy data.

[21] 9. Evaporite Mineralogy – Data set(s) required: VNIR and/or TIR field spectra. 0 = No diagnostic sulfate or carbonate absorption features identified in field spectra; linear deconvolution results do not include these compositions. 1 = Shallow diagnostic absorption features, concentrations of <35% indicated by linear deconvolution (see Bound/Interlayer Water description for rationale). May also be applied where linear deconvolution does not indicate evaporite composition but visual inspection does; also where noisy field spectra make analysis difficult. 2 = Distinct diagnostic absorption features and/or significant concentrations (>35%) implied by linear deconvolution. Notes: Certain salt mineralogies (e.g., halite) have no diagnostic spectral features in either instrument range.

[22] 10. Fog Deposition (regional)* – Data set(s) required: SPI, navcams, orbital topography. Scoring: method identical to orbitally derived fog deposition, but additionally includes the visible identification of fog in rover imagery. Notes: Need single, good SPI panorama + orbital DEM and applies to single locale—score strengthened by repeated observations, observations as a function of time. Score = 2 needs >1 observation.

[23] 11. Hydrologic Geomorphology* – Data set(s) required: SPI panoramas; navcam images within field of view at locale. 0 = No geomorphic evidence of hydrologic and/or hydrogeologic activity. 1 = Some indicators of hydrologic and hydrogeologic activity present (e.g., polygonal or patterned terrain, visible paleodrainages). 2 = increased frequency and diversity of geomorphic indicators that collectively point to hydrologic and/or hydrogeologic activity.

[24] 12. Insolation* – Data set(s) required: Vis-band imaging and/or rover weather station pyranometer. 0 = Full sunlight environments, e.g., open plains, full sun from weather data. 1 = Environments with periodic shelter from sun, e.g., shaded hillslopes, incised channels or valleys, clouds or intermittent break from sun in concurrent weather data. 2 = Environments with frequent shelter from sun, as described above but with positive indication from multiple hypotheses in 1.

[25] 13. Moisture (locale)* – Data set(s) required: FI and all cameras. 0 = No visible moisture in soils, on rocks from SPI or FI images. 1 = Not applicable; binary variable. 2 = Visible soil moisture patches and/or liquid water on rocks. Notes: This variable follows from early morning imaging campaigns targeting the direct observation of local, overnight condensation or ponding of atmospheric water vapor.

[26] 14. Moisture (regional)* – Data set(s) required: SPI, navcams. 0 = No visible evidence for moisture (e.g., no visible fog from pan-based during several sols). 1 = Areas, locales, features that have visible fog/clouds/snow. 2 = Consistent identification of clouds/fog/snow at the specific location, elevation, feature of the applicable locale indicating the consistent presence and potential availability of water. Notes: Need single, good SPI panorama and applies to single locale—score strengthened by multiple observations, observations as a function of time.

[27] 15. Promising Habitat* – Data set(s) required: FI and all cameras. 0 = Identification of desert habitats that generally have decreased biological abundance (e.g., low albedo desert pavement) in comparison to other habitats; no feature in rover imagery that appears conducive for life. 1 = Habitats are present similar to those known to be generally conducive for life, such as alluvial fans for lithophytic microbes, but with additional corroborating data from FI and other cameras, such as small hills (for moisture to collect) or surfaces with what appear to be more porous materials. Often in these habitats abundance may be patchy, widely dispersed or difficult to detect. 2 = Identification of habitats known in terrestrial and Mars analog deserts to be particularly conducive to life, including hypersaline habitats, playas, lake beds, drainage channels or alluvial fans with significant heterogeneity in rock size and albedo, quartz fields, hot springs, etc. Notes: factor scoring scaled to desert habitats and is subjective to observer's experience and methodology in similar environments.

[28] 16. Quartz – Data set(s) required: TIR field spectra. 0 = No quartz identified by linear deconvolution; no quartz diagnostic features visible in TIR. 1 = Low (<35%) concentrations of quartz identified by linear deconvolution, or visual identification of diagnostic quartz absorption features without confirmation by linear deconvolution. May also apply if significant amounts of silica-rich non-quartz material (obsidian, for example) are indicated, or if quartz is subjectively identified in VNIR spectra. 2 = High concentrations (>35%) of quartz identified by linear deconvolution. Notes: Quartz has no diagnostic spectral features in the VNIR.

[29] 17. Relative Humidity – Data set(s) required: overnight EnviS relative humidity (RH). 0 = RH < 75%. 1 = 75% < RH < 90%; 75% based approximately on lower limit for atmospheric water utility by lichens. 2 = 90% < RH < 100%; 90% liberal estimate of when liquid water droplets form in the air, becoming bioavailable. Notes: Overnight relative humidity applied to morning locale, previous night's locale, and locales at same elevation within ~500 m radius.

[30] 18. Water Vapor Condensation – Data set(s) required: overnight EnviS (a) leaf wetness (LW) sensor voltage and (b) air temperature, dewpoint temperature (from RH). 0 = V < 0.5, air temperature > dewpoint temperature this is the dry value for the sensor. 1 = 0.5 < V < 1.0; intermediate to wet value, below: physically a thin film of water. 2 = V > 1.0, air temperature $\leq$ dewpoint temperature; physically water droplets condensed on surface. Notes: (b) is a binary rating factor, redundant to (a) and only applies to scores of 0 and 2 below if needed (e.g., dew sensor not functional, or data is questionable). Scoring applied to locales as described for Relative Humidity, above.

3.2.2. Scoring Biological Variables

[31] Biology variables are scored using data from the rover's fluorescence imager, described in further detail by

Weinstein et al. [2007]. Briefly, the system employs a sophisticated camera and flash arrangement to make high resolution color images of the field of view directly beneath the rover. Critical for this study, it also has the capability to spray biomolecule specific fluorescent dyes on the surface, revealing the presence or absence of carbohydrates, chlorophyll, DNA, lipids, or proteins and, along with other lines of evidence, support or refute the biological hypothesis. Variable 1 in Table 3, Morphology, is the only biological variable that employs no dyes and is entirely non-quantitative, but instead based on the data user's experience with and past observations of desert life. Variables 2–6 represent the findings of the five aforementioned fluorescence channels.

[32] 1. Morphology* – Data set(s) required: FI, all cameras. 0 = Nothing in the FI field-of-view (FOV) shows a morphology indicative of life (e.g., lichens, cyanobacterial colonies, macroscopic organisms). 1 = Morphology has features that can be associated with life but may be from a different source (e.g., a green band imaged on a rock, ambiguously microbial or mineralogical in origin). 2 = Definitive morphology of life detected. Notes: Scoring based on all cameras: visual biosignature anywhere in a panorama, anywhere in a RGB FI or up to 180 m prior to locale in navcam images.

[33] 2–6. Carbohydrate, chlorophyll, DNA, lipid, protein – Data set(s) required: FI. 0 = No fluorescence signal in any region of the FOV. 1 = Weak signal to noise or ambiguous origin (e.g., light albedo, ambient light in the image, mineral fluorescence). Also in consideration is when the scale factor on the images is greater than or equal to one, indicating a contrast stretched image set. 2 = Bright signal on some region(s). Notes: Signals are measured from a comparison of images prior to and following application of relevant dyes. Single pixel signals will be discarded as random noise. Chlorophyll only: fluorescence in this channel may be evident before application of water or dyes—in such a case, a comparison with the RGB and dye imagesis necessary.

3.2.3. Application

[34] In order to integrate data collection and generate standard metrics of potential habitability and life detection, the scores from each studied locale were tallied and represented as ratio scores, named *Renv* and *Rbio*, respectively. These values were calculated for a given locale by (1) summing all available environmental and biological scores (based on relevant data collection) and (2) dividing the sum by the total possible (also a function of payload deployment and relevant data collection). In theory, the maximum score for the biological and environmental elements at a given locale is 36 and 10, respectively. In practice, however, the maximum element score varies as a function of instrument deployment and data collection. To account for this variability, we divide the total environmental and biological scores by the maximum possible at the respective locale. Thus, all available data regarding habitability and life are integrated to a single standard value, or ratio score, ranging from 0 to 1. All data on individual variables was retained, but this calculation provided the means to enhance traverse planning and target selection by allowing the remote science team to quickly compare and visualize differences between locales and sites.

[35] For the environmental element, this value is named *Renv*, represents the potential habitability as constrained by the rover's payload and as defined by the variables in Table 2: 0 indicates low potential habitability, while 1 indicates high potential habitability. The environmental scoring element was designed such that, in a global context, most terrestrial biomes, such as grasslands and forests, would reliably produce a value of *Renv* approaching 1, while a generally inhospitable landscape such as the Atacama Desert (or perhaps the martian landscape) would exhibit some value between 0 and 1. In the assessment of biology, *Rbio* represents the strength of evidence for life as defined by the rover's fluorescence imager and visible-band cameras (Table 3): 0 indicates weak or no evidence for life while 1 indicates strong evidence for life. As with the environmental element, the biological element follows from the rover's payload and is thus tailored to the desert environment, in analogy to Mars. Therefore, we expected that *Rbio* would theoretically approach a value of one for the majority of terrestrial ecosystems but exhibit some variation throughout our study. Despite the assertion that some observations may reflect potential habitability or the presence of biology more significantly than others, establishing a weighting scheme was beyond the scope of this work and each variable score was weighted equally.

[36] Mapping the results of the DSS was accomplished with orbitally derived digital elevation maps and imagery and the Eventscope software package (P. Coppin et al., unpublished manuscript, 2007). There, environmental scores were used to color code map ''pins'' which illustrated locales visited by the rover along its traverse. Biology scores were used as pins' text labels. In this manner, we were able to visualize predicted habitability and our confidence in biological detection in a single data product, ultimately mapping the distribution of habitats and life in the Atacama (see Figure 1 and *Cabrol et al.* [2007] for examples).

4. Results

[37] Here we present results from the scoring system developed and tested during the 2005 LITA field experiment at Sites D, E, and F. Over all three sites, the rover completed investigation of 106 locales. Regional investigations were initially targeted by analysis of orbital data prior to field activities and local scale investigations were subsequently refined by data returned from the rover. Fifty-seven of those, or approximately 54% of the visited locales, were scored for both environment and biology. Because multiple investigations were carried out at many locales, and transect waypoints were enumerated by a single locale number, this represents a total of $N = 171$ independent samples. However, as the availability of relevant data varied as a function of data quality and the subset of instruments deployed at each locale, so only four samples were scored for every environmental and biological variable. The ratios *Renv* and *Rbio* were used to account for this and characterize the relative habitability and biology detection of each sample.

4.1. Indicators of Habitability and Life

[38] How is life detection related to potential habitability? Figures 3–5 show this relationship in the Atacama Desert

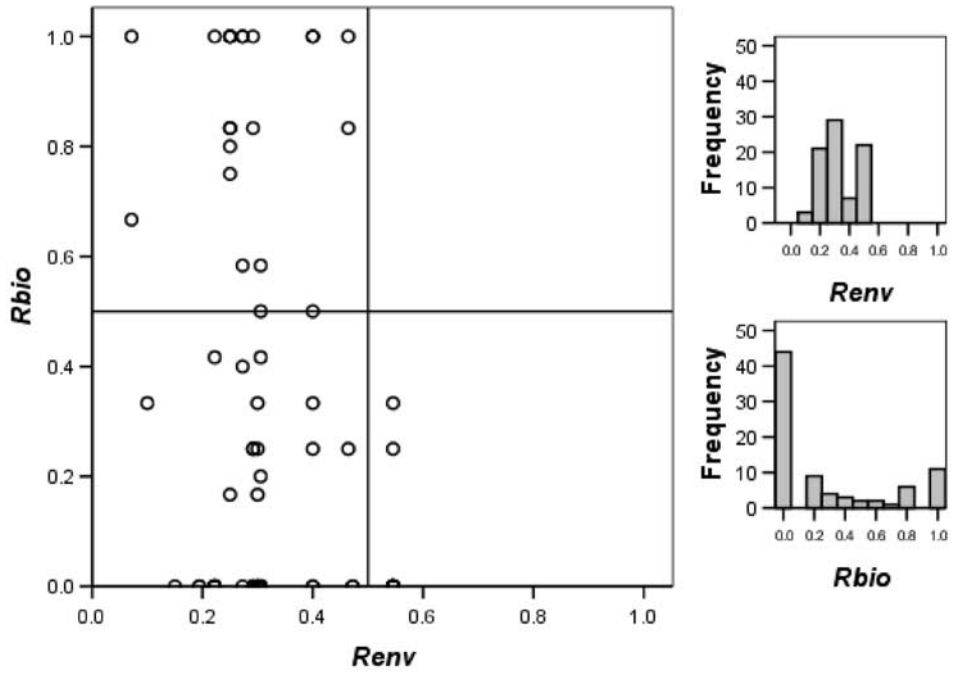

Figure 3. Biology and environment scores and frequencies from the locales of LITA Site D. Potential habitability increases to the right along the *Renv* axis; strength of evidence for life increases upward on the *Rbio* axis. $N = 82$ samples; mean *Renv* (σ) = 0.34(0.13); Mean *Rbio* (σ) = 0.28(0.38). Reference lines *Renv* = 0.5 and *Rbio* = 0.5 delineate four quadrants that represent relatively inhospitable locales with stronger evidence for life (top left) and weaker evidence for life (bottom left); relatively hospitable locales with stronger evidence for life (top right) and weaker evidence for life (bottom right).

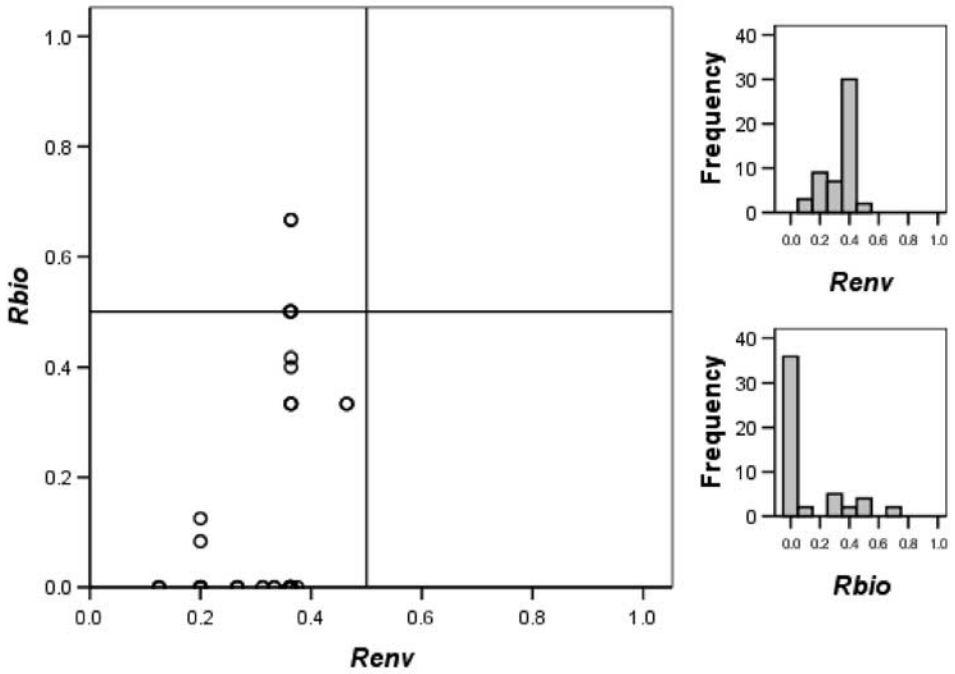

Figure 4. Biology and environment scores and frequencies from the locales of LITA Site E. Potential habitability increases to the right along the *Renv* axis; strength of evidence for life increases upward on the *Rbio* axis. $N = 51$ samples; mean *Renv* (σ) = 0.32(0.08); Mean *Rbio* (σ) = 0.12(0.20). Reference lines *Renv* = 0.5 and *Rbio* = 0.5 delineate four quadrants that represent relatively inhospitable locales with stronger evidence for life (top left) and weaker evidence for life (bottom left); relatively hospitable locales with stronger evidence for life (top right) and weaker evidence for life (bottom right).

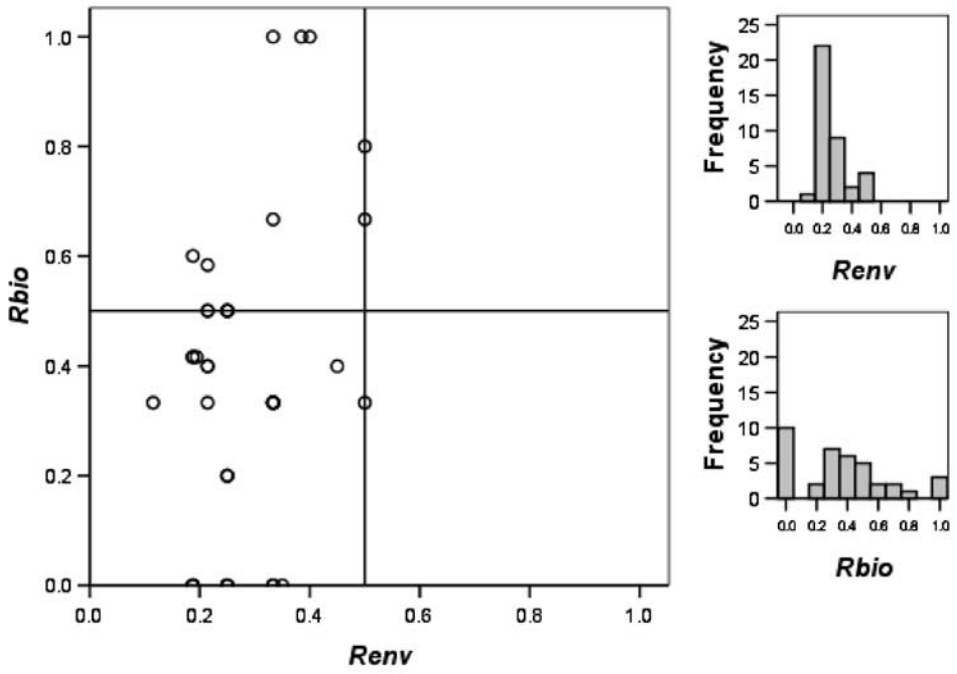

Figure 5. Biology and environment scores and frequencies from the locales of LITA Site F. Potential habitability increases to the right along the *Renv* axis; strength of evidence for life increases upward on the *Rbio* axis. $N = 38$ samples; mean *Renv* (σ) = 0.28(0.10); Mean *Rbio* (σ) = 0.37(0.29). Reference lines *Renv* = 0.5 and *Rbio* = 0.5 delineate four quadrants that represent relatively inhospitable locales with stronger evidence for life (top left) and weaker evidence for life (bottom left); relatively hospitable locales with stronger evidence for life (top right) and weaker evidence for life (bottom right).

by plotting *Rbio* versus *Renv* for the three field sites. With generally low values for *Renv*, results from the scoring system suggest that the locales within sites D–F are relatively inhospitable (Table 4). The vast majority (88%) had *Renv* < 0.5 and average values of *Renv* range from 0.28 ± 0.10 at site F, increasing to a maximum of 0.34 ± 0.13 at site D. Average values for biology ratio, *Rbio*, range from 0.12 ± 0.20 at site E to 0.37 ± 0.29 at site F, but the high standard deviation of these measurements—particularly at site E—requires the acquisition of more samples to calculate a more statistically robust relationship.

4.2. Correlations

[39] The Pearson linear correlation coefficient, *r*, was first calculated between values of *Renv* and *Rbio* across all locales from all sites to investigate the validity of the hypothesis that a system such as the DSS may be used to guide robotic exploration for life in a Mars-like desert environment. At sites E and F, *Renv* and *Rbio* vary together ($r = 0.376$ and 0.361, respectively), while at site D, the correlation is weakly negative ($r = -0.286$). At site D, the negative correlation may be partly explained by exploration strategy: early in the 2005 field season, the remote science team employed a strategy that included abbreviated investigations of more locales, a strategy that did not allow for the uniform deployment of the dye-bearing FI experiments. Thus, identification of strong evidence for life may not be well represented. The positive correlations for sites E and F, however, support the hypothesis that environmental variables may be used to delineate zones of habitability and guide the robotic exploration for life. Although these values are far less than one, a positive correlation nonetheless indicates that the basis of our hypotheses bore positive results. By continuing to tune our payload- and ecosystem-defined metrics of habitability and continuing to retrieve more frequent and uniform data on local biology, we expect this correlation to strengthen in future missions. In the future, developing a weighting system for particularly relevant biological or environmental variables may also be appropriate.

[40] Table 5 shows the correlation amongst environmental variables and the *Rbio* ratio. Owing to the small number of biology variables and sparseness of their measurements, the inverse correlations, those between biological variables and *Renv*, could not be calculated. Interestingly, the four strongest positive correlations associated with evidence for life were derived from spectral data: Field Chlorophyll ($r =$

Table 4. Descriptive Statistics From the LITA Data Scoring System at Sites D, E, and F[a]

	Site D	Site E	Site F
Sample number, *N*	82	51	38
Mean *Renv* (σ)	0.34 (0.13)	0.32 (0.08)	0.28 (0.10)
Mean *Rbio* (σ)	0.28 (0.38)	0.12 (0.20)	0.37 (0.29)
Renv-*Rbio* correlation, *r*	−0.286[b]	0.376[b]	0.361[c]

[a] *Renv* and *Rbio* are the environment and biology score ratios, respectively, or the total score divided by the maximum possible considering all available data.
[b] The correlation is significant at the 0.01 level.
[c] The correlation is significant at the 0.05 level.

Table 5. Environmental Variable Correlation With Biology Ratio, *Rbio*, Over Sites D, E, and F

Variable	*R*
Orbital	
Atmospheric Water	0.017
Chlorophyll	n/a[a]
Evaporite Mineralogy	0.186[b]
Fog Deposition	−0.190[b]
Hydrologic Geomorphology	−0.132
Quartz	−0.003
Field	
Bound/Interlayer Water	0.160
Chlorophyll	0.283[b]
Evaporite Mineralogy	0.166
Fog Deposition (regional)	−0.210[b]
Hydrologic Geomorphology	−0.028
Insolation	0.061
Moisture (locale)	n/a
Moisture (regional)	−0.056
Promising Habitat	0.049
Quartz	0.092
Relative Humidity	−0.172
Water Vapor Condensation	−0.156

[a]The correlation could not be calculated due to missing data.
[b]The correlation is significant at the 0.05 level.

0.283), Orbital Evaporite Mineralogy (r = 0.186), Field Evaporite Mineralogy (r = 0.168), and Field Bound/Interlayer Water (r = 0.160). Although these correlations are only weakly positive, they warrant further investigation and support the continued use of spectral instruments in the robotic search for life. Specifically, these values stress the need for the collection of more complete biological data sets at each locale, since only 45 of the 171 total samples taken across the three sites had data on all biological variables. The two strongest negative correlations, Field Fog Deposition (r = −0.210) and Orbital Fog Deposition (r = −0.190) were both derived from topographic data or inferences from visible band imagery regarding the deposition of atmospheric water on the surface. In turn, these suggest that we may need to alter our assumptions regarding the mechanism or frequency of fog deposition due to local topography, or perhaps the bioavailability of this water source. Pairwise calculation of the correlation coefficient could not be made for two variables, Orbital Chlorophyll and Field Moisture (locale), due to missing data.

4.3. Factor Analysis

[41] Factor analysis is a common data reduction technique of multivariate statistics by which groups of correlated variables that represent a common underlying dimension, or factor, are isolated from a larger set of original variables (e.g., Kachigan, 1991). We performed factor analysis of the scoring system environment and biology variables with the aim of (a) identifying underlying factors responsible for the observed variability in habitat and biology; (b) screening the scoring system for redundant variables, representative of increased cost in mass and energy to a planetary mission, for future experiments. All calculations presented here were completed using SPSS 14.0 statistics software (SPSS, 2005). In both of the following cases, factors were extracted by principal component analysis, those with initial eigenvalues greater than one were retained, and rotation of the initial component matrix was accomplished by varimax rotation with Kaiser normalization.

[42] Scores across all locales and samples from fourteen of the eighteen environmental variables presented in Table 2 were employed in the following factor analysis (Table 6). Two, orbital chlorophyll and field moisture (locale-scale), exhibited zero variance, while correlation coefficients could not be calculated between field chlorophyll and field fog deposition due to the anticorrelation of missing data between the two sets (that is, where observations were taken on fog, chlorophyll data was not available often enough for robust conclusions to be drawn about their correlation, and vice versa). Of the fourteen initial environmental variables input for this analysis, five underlying factors were identified that cumulatively explained 96.2% of all observed variance. Importantly, the results of this analysis address one of the main goals of this work by illustrating which environmental factors exert the most influence on habitability in a desert ecosystem. As seen in factor I, 30.1% of the observed variance is effectively explained by variables that largely relate to the physical and chemical properties of the surface, or potential substrate for life. Factor II explains 23.8% of the total variance with variables associated with atmospheric water condensation (dew); notably, negative factor loadings are shown for variables derived from surface properties. Orbital indicators of atmospheric water vapor transport control the third factor. Factor IV (15.1%) appears to group a diverse set of variables whose common thread is

Table 6. Factor Analysis Summary for Sites D–F Environmental (Habitat) Scoring

Factor Names and High-Loading Variables	Factor Loadings	%Variance Explained	Cumulative, %
Factor I: Substrate		30.1	30.1
Field Bound/Interlayer Water	0.97		
Moisture (regional)	0.97		
Promising Habitat	0.91		
Orbital Hydrologic Geomorphology	0.84		
Orbital Quartz	0.39		
Orbital Evaporite	0.30		
Factor II: Dew		23.8	53.9
Relative Humidity	0.94		
Water Vapor Condensation	0.84		
Orbital Fog Deposition	0.48		
Field Hydrologic Geomorphology	0.48		
(Field Quartz)	−0.57		
(Orbital Evaporite)	−0.92		
Factor III: Clouds, Fog		18.2	72.1
Orbital Atmospheric Water	0.96		
Orbital Fog Deposition	0.71		
(Field Quartz)	−0.51		
(Orbital Quartz)	−0.87		
Factor IV		15.1	87.2
Insolation	0.94		
Field Hydrologic Geomorphology	0.60		
Field Quartz	0.54		
(Field Water Vapor Condensation)	−0.42		
Factor V: Evaporite		9.0	96.2
Field Evaporite	0.97		
Promising Habitat	0.36		

Table 7. Factor Analysis Summary for Sites D–F Biology Scoring

Factor Names and High-Loading Variables	Rotated Factor Loading	% Variance Explained	Cumulative, %
Factor I:		31.2	31.2
Morphology	0.96		
Chlorophyll	0.95		
Factor II:		25.7	56.9
Protein	0.93		
Lipid	0.72		
DNA	0.33		
Factor III:		23.0	79.9
Carbohydrate	0.92		
DNA	0.60		
Lipid	0.38		

a weak anticorrelation with variables associated with contemporary water availability, particularly water derived from the atmosphere. Factor V (9.0%) illustrates the unique role that evaporite mineralogy has in implicating potentially habitable desert environments.

[43] Factor analysis of the scoring system biology variables revealed three underlying factors, or in this case genres of life detection, that collectively explain 79.9% of the observed variance across sites D, E and F (Table 7). The first genre of life detection, represented by factor I, is based nearly equally on visible morphology and chlorophyll fluorescence. Their minor contributions to other factors and strong correlation to one another (r = 0.84) suggests some redundancy: for example, if one or the other mode of data acquisition were incapacitated, detection by either chlorophyll or morphology would still result in a unique detection. The second and third genres of life detection illustrated by this analysis are detection by protein and carbohydrate fluorescence, respectively. Both factors II and III, which together explain nearly half of all observed variance, have high-loading contributions from DNA and lipid fluorescence, as well, but the unique discriminator between them is the contribution of protein in factor II (rotated factor loading = 0.93), the contribution of carbohydrate in factor III (rotated factor loading = 0.92). In summary, we postulate that these three genres of life detection represent fundamentally different responses to the FI system experiments.

5. Discussion

[44] The environmental and biological ratios, *Renv* and *Rbio* were defined such that missing data was accounted for and from Figures 3–5 we see that *Renv* was less than 0.5 for nearly all locales, indicating a low potential habitability for the Atacama, in general. *Renv* appears to increase slightly with increasing proximity to the coast, but this variation is within the standard deviation of the calculated values and requires more temporal and geographic coverage of climate data. *Renv* and *Rbio* were positively correlated for sites E and F, suggesting that potential habitability may be an effective predictor of life detection. However, the correlations are relatively weak and the correlation was negative for site D, prompting continued experimentation.

[45] Interestingly, we found that the four environmental variables with the strongest correlation to *Rbio* were all derived from field and orbital spectral data, arguing for the continued use of spectral instruments for aboard astrobiological missions. The two strongest negative correlations were with environmental variables describing the topographic potential for fog embankment, suggesting either (a) that we reconsider their inclusion as a predictive measure in future systems, (b) that we develop a more robust/quantitative model of its relationship to life in desert environments, including the possibility of weighting this and other factors in anticipation of subsequent deployments. On the other hand, these preliminary findings require further ground truth.

[46] Currently, the scoring system applies no weighting to variable values. However, factor analysis of environmental and biological variables illustrated several interesting underlying trends. Five factors, interpreted as environmental constraints on habitability, were extracted from 14 original environmental variables. Three biological factors were identified from six original variables: in this case, the factors appeared to group variables associated with genres of life detection, or possibly different types of organisms. For example, one would expect chlorophyll-bearing organisms to be more readily identified by chlorophyll detection compared to those that may only be identified by morphology or other biomolecule fluorescence. The most significant factor in the variance of biological detection across sites is driven by morphological evidence and observations of chlorophyll fluorescence. The second two factors in this analysis differ mostly by their primary factors: detection by protein fluorescence versus detection by lipid fluorescence. These three could represent the detection of similar organisms on different substrates, where detection by other means could be limited or faulty; alternatively, they could represent different types of organisms. Results from ground truth experiments in the future will be capable of making this distinction. In future versions of the scoring system, weighting may be applied to variables based on rotated factor loadings from controlled field investigations.

[47] Several lessons from the results of this study may be applied to future exploration and data scoring:

[48] 1. A system with fewer, more quantitatively defined environmental variables would likely (a) capture much of the observed variability in potential habitability and (b) allow for a more controlled investigation of the correlation between postulated habitability and biological detection.

[49] 2. Statistical patterns in the correlation between individual environmental and biological variables would be strengthened in future analysis by uniform payload deployment. Although this is an unlikely scenario during live mission activities, independent study of these relationships would benefit targeting at all spatial scales.

[50] 3. Both correlation and factor analysis suggest a simplification of the scoring scheme. Three genres, or modes of life detection were found to underlie most of the observed variability in biological detection with the fluorescence imager and 5 environmental factors were found to underlie most of the observed variability in potential habitability.

6. Conclusions and Implications

[51] Remote exploration of life through orbital and rover field based reconnaissance conducted during the LITA

experiment represents a step forward in preparing for the astrobiological robotic exploration of Mars. Here, we have presented the development and first deployment of a tool to help identify the environmental factors controlling habitability in a Mars analog terrestrial desert and a mode for evaluating its capabilities. Following continued research, such environmental factors may be used to target rover-based life detection experiments. Future work will focus on continuing development of this method not only as a method to integrate data and streamline top-level analysis, but also as a method for predicting the location of habitable environments and potential refuges for life in desert environments on Earth and Mars.

[52] **Acknowledgments.** This Life in the Atacama project was supported by the NASA ASTEP program, grant NAG5-12890. The authors wish to acknowledge the insightful comments of two anonymous reviewers, as well as the invaluable contributions of all project team members.

References

Arvidson, R. E., et al. (1998), Rocky 7 prototype Mars rover field geology experiments: 1. Lavic Lake and Sunshine Volcanic Field, California, *J. Geophys. Res.*, *103*, 22,671–22,688.

Arvidson, R. E., S. W. Squyres, E. Baumgartner, P. Schenker, C. Niebur, K. Larsen, F. Seelos, N. Snider, and B. Jolliff (2002), FIDO prototype Mars rover field trials, Black Rock Summit, Nevada, as test of the ability of robotic mobility systems to conduct field science, *J. Geophys. Res.*, *107*(E9), 8002, doi:10.1029/2000JE001464.

Baker, V. R. (2001), Water and the Martian landscape, *Nature*, *412*, 228–236.

Baker, V. R., R. G. Strom, V. C. Gulick, J. S. Kargel, G. Komatsu, and V. S. Kale (1991), Ancient oceans, ice sheets and the hydrological cycle on Mars, *Nature*, *352*, 589–594.

Cabrol, N. A., et al. (2001a), Science results of the Atacama Nomad rover field experiment, Chile: Implications for planetary exploration, *J. Geophys. Res.*, *106*(E4), 7664–7675.

Cabrol, N. A., D. D. Wynn-Williams, D. A. Crawford, and E. A. Grin (2001b), Recent aqueous environments in Martian impact craters: An astrobiological perspective, *Icarus*, *154*, 98–113.

Cabrol, N. A., et al. (2007), Life in the Atacama: Searching for life with rovers (science overview), *J. Geophys. Res.*, *112*, G04S02, doi:10.1029/2006JG000298.

Chong Diaz, G., M. Mendoza, J. Garcia-Veigas, J. J. Pueyo, and P. Turner (1999), Evolution and geochemical signatures in a Neogene forearc evaporitic basin: The Salar Grande (Central Andes of Chile), *Paleogeogr. Paleoclimatol. Paleoecol.*, *151*, 39–54.

Christensen, P. R., et al. (2001), The Mars Global Surveyor Thermal Emission Spectrometer experiment: Investigation description and surface science results, *J. Geophys. Res.*, *106*, 23,823–23,871.

Dohm, J. M., J. C. Ferris, V. R. Baker, R. C. Anderson, T. M. Hare, R. G. Strom, N. G. Barlow, K. L. Tanaka, J. E. Klemaszewski, and D. H. Scott (2001a), Ancient drainage basin of the Tharsis region, Mars: Potential source for outflow channel systems and putative oceans or paleolakes, *J. Geophys. Res.*, *106*, 32,943–32,958.

Dohm, J. M., et al. (2001b), Latent activity for western Tharsis, Mars: Significant flood record exposed, *J. Geophys. Res.*, *106*, 12,301–12,314.

Dohm, J. M., K. L. Tanaka, and T. M. Hare (2001c), Geologic map of the Thaumasia region of Mars, *U.S. Geol. Surv. Map*, *I-2650*.

Dohm, J. M., J. C. Ferris, N. G. Barlow, V. R. Baker, W. C. Mahaney, R. C. Anderson, and T. M. Hare (2004), The Northwestern Slope Valleys (NSVs) region, Mars: A prime candidate site for the future exploration of Mars, *Planet. Space Sci.*, *52*, 189–198.

Fairén, A. G., J. M. Dohm, V. R. Baker, M. A. de Pablo, J. Ruiz, J. C. Ferris, and R. C. Anderson (2003), Episodic flood inundations of the northern plains of Mars, *Icarus*, *165*, 53–67.

Fink, W., J. M. Dohm, M. A. Tarbell, T. M. Hare, and V. R. Baker (2005), Next-generation robotic planetary reconnaissance missions: A paradigm shift, *Planet. Space Sci.*, *53*, 1419–1426.

Furfaro, R., J. M. Dohm, W. Fink, D. Schulze-Makuch, A. G. Fairén, M. A. Tarbell, T. M. Hare, and V. R. Baker (2006), Multi-layer fuzzy logic-based expert system for conducting tier scalable planetary reconnaissance [abstract 1257], in *Proceedings of 37th Lunar and Planetary Science Conference Abstracts* [CD-ROM], Lunar and Planet. Inst., Houston, Tex.

Gendrin, A., N. Mangold, J. P. Bibring, Y. Langevin, B. Gondet, F. Poulet, G. Bonello, C. Quantin, J. Mustard, R. Arvidson, and S. LeMouelic (2005), Sulfates in Martian layered terrains: The OMEGA/Mars Express view, *Science*, *307*, 1587–1591.

Márquez, A., C. Fernández, F. Anguita, A. Farelo, J. Anguita, and M.-A. de la Casa (2004), New evidence for a volcanically, tectonically, and climatically active Mars, *Icarus*, *172*, 573–581.

McSween, H. Y., et al. (2006), Characterization and petrologic interpretation of olivine-rich basalts at Gusev Crater, Mars, *J. Geophys. Res.*, *111*, E02S10, doi:10.1029/2005JE002477.

Mouginis-Mark, P. J. (1985), Volcano/ground ice interactions in Elysium Planitia, Mars, *Icarus*, *64*, 265–284.

Mouginis-Mark, P. J. (1990), Recent water release in the Tharsis region of Mars, *Icarus*, *84*, 362–373.

Neukum, G., et al. (2004), Recent and episodic volcanic and glacial activity on Mars revealed by the High Resolution Stereo Camera, *Nature*, *432*, 971–979.

Piatek, J. L., et al. (2007), Surface and subsurface composition of the Life in the Atacama field sites from rover data and orbital image analysis, *J. Geophys. Res.*, *112*, G04S04, doi:10.1029/2006JG000317.

Riquelme, R., J. Martinod, G. Hérail, J. Darrozes, and R. Charrier (2003), A geomorphological approach to determining the Neogene to Recent tectonic deformation in the Coastal Cordillera, *Tectonophysics*, *361*, 255–275.

Schulze-Makuch, D., J. M. Dohm, A. G. Fairén, V. R. Baker, W. Fink, and R. G. Strom (2005), Venus, Mars, and the ices on Mercury and the Moon: Astrobiological implications and proposed mission designs, *Astrobiology*, *5*, 778–795.

Schulze-Makuch, D., J. M. Dohm, C. Fan, A. G. Fairén, J. A. P. Rodriguez, V. R. Baker, and W. Fink (2007), Exploration of hydrothermal targets on Mars, *Icarus*, *189*(2), 308–324.

Scott, D. H., J. M. Dohm, and D. J. Applebee (1993), Geologic map of science study area 8, Apollinaris Patera region of Mars, *U.S. Geol. Surv. Misc. Invest. Ser. Map*, *I-2351* (*1:500,000*).

Scott, D. H., J. M. Dohm, and J. W. Rice Jr. (1995). Map of Mars showing channels and possible paleolake basins, *U.S. Geol. Surv. Misc. Invest. Ser. Map*, *I-2461* (*1:30,000,000*).

Squyres, S. W., et al. (2004), In situ evidence for an ancient aqueous environment at Meridiani Planum, Mars, *Science*, *306*, 1709.

Stoker, C. R., et al. (2001), Marsokhod Rover Mission simulation at Silver Lake, California, 2000: Mission overview, *J. Geophys. Res.*, *106*(E4), 7639–7664.

Tanaka, K. L., J. M. Dohm, J. H. Lias, and T. M. Hare (1998), Erosional valleys in the Thaumasia region of Mars: Hydrothermal and seismic origins, *J. Geophys. Res.*, *103*, 31,407–31,419.

Tanaka, K. L., J. A. Skinner Jr., and T. M. Hare (2005), Geologic map of the northern plains of Mars, *U.S. Geol. Surv. Misc. Invest. Ser. Map*, *SIM-2888* (*1:15,000,000*).

Warren-Rhodes, K., et al. (2007a), Searching for microbial life remotely: Satellite-to-rover habitat mapping in the Atacama Desert, Chile, *J. Geophys. Res.*, *112*, G04S05, doi:10.1029/2006JG000283.

Warren-Rhodes, K., et al. (2007b), Robotic ecological mapping: Habitats and the search for life in the Atacama Desert, *J. Geophys. Res.*, *112*, G04S06, doi:10.1029/2006JG000301.

Weinstein, S., et al. (2006), Implementation of a daylight fluorescence imaging system to autonomously detect biomarkers of extant life in the Atacama Desert, paper presented at 37th Lunar and Planetary Science Conference, League City, Tex., 13–17 March.

Weinstein, S., et al. (2007), Application of pulsed-excitation fluorescence imager for daylight detection of sparse life in tests in the Atacama Desert, *J. Geophys. Res.*, doi:10.1029/2006JG000319, in press.

Wettergreen, D., D. Bapna, M. Maimone, and G. Thomas (1999), Developing Nomad for robotic exploration of the Atacama Desert, *Robotics Auton. Syst. J.*, *26*(2–3), 127–148.

Wettergreen, D. S., et al. (2005a), First experiments in the robotic investigation of life in the Atacama Desert of Chile, paper presented at International Conference on Robotics and Automation, Inst. of Electr. and Electron. Eng., Barcelona.

Wettergreen, D. S., et al. (2005b), Second experiment in the robotic investigation of life in the Atacama Desert of Chile, paper presented at International Symposium on Artificial Intelligence, Robotics and Automation in Space (iSAIRAS), Munich, Germany.

N. A. Cabrol, E. A. Grin, and K. Warren-Rhodes, Space Science Division, NASA Ames Research Center, MS 245-3, Moffett Field, CA 94035-1000, USA.

C. S. Cockell, Planetary and Space Sciences Research Institute, Open University, Milton Keynes MK7 6AA, UK.

P. Coppin, Eventscope, Remote Experience and Learning Laboratory, Studio for Creative Inquiry, Carnegie Mellon University, 4615 Forbes Avenue, Suite 110, Pittsburgh, PA 15217, USA.

J. M. Dohm, Hydrology and Water Resources Department, University of Arizona, Tucson, AZ 85721, USA.

L. Ernst, G. Fisher, E. Minkley, A. Waggoner, and S. Weinstein, Molecular Biosensor and Imaging Center, Mellon Institute, Carnegie Mellon University, 4400 5th Avenue, Pittsburgh, PA 15213, USA.

J. Glasgow, E. Pudenz, and G. Thomas, GROK Laboratory, University of Iowa, Iowa City, IA 52242, USA.

C. Hardgrove, J. Moersch, J. Piatek, and M. Wyatt, Department of Earth and Planetary Sciences, University of Tennessee, Knoxville, TN 37996, USA.

A. N. Hock, Department of Earth and Space Sciences, University of California, Los Angeles, Los Angeles, CA 90095, USA.

D. Jonak, T. Smith, K. Stubbs, D. Thompson, M. Wagner, and D. S. Wettergreen, Robotics Institute, Carnegie Mellon University, 5000 Forbes Avenue, Pittsburgh, PA 15213, USA.

L. Marinangeli and G. G. Ori, International Research School of Planetary Sciences, I-65127 Pescara, Italy.